  Bul. Chem. Soc. Jpn., 55, 3603—3606 (1982)

Studies on Salt Hydrate for Latent Heat Storage. I. Crystal Nucleation of Sodium Acetate Trihydrate Catalyzed by Tetrasodium Pyrophosphate Decahydrate

Takahiro WADA* and Ryoichi YAMAMOTO

Material Research Laboratory, Matsushita Electric Industrial Co., Ltd., Kadoma, Osaka 571

(Received April 2, 1982)

The effect of tetrasodium pyrophosphate decahydrate ($Na_4P_2O_7 \cdot 10H_2O$) as a nucleation catalyst for sodium acetate trihydrate ($CH_3CO_2Na \cdot 3H_2O$) is shown. The supercooled melt of 10 g of $CH_3CO_2Na \cdot 3H_2O$ recrystallized at about 5 degrees below the melting point only when 0.1 g of $Na_4P_2O_7 \cdot 10H_2O$ was added to it. More than a thousand cycles of alternate heating and cooling through the melting point were carried out in this work. Some observations on nucleation are given and the results are discussed on the basis of crystallographic data.

Sodium acetate trihydrate ($CH_3CO_2Na \cdot 3H_2O$) has received attention recently because of its large latent heat of fusion (about 264 J/g) which makes it attractive as a latent heat storage material.[1] But once this material melts, it tends to supercool even if it is cooled considerably below the melting point (58.4 °C).[2] One approach to this problem is to add a suitable nucleation catalyst to supercooled $CH_3CO_2Na \cdot 3H_2O$ melt. This nucleation catalyst needs to be hardly soluble in $CH_3CO_2Na \cdot 3H_2O$ melt so as to not lower the melting point nor diminish the heat of fusion.[3] However, such a nucleation catalyst has not been found yet.[4,5] In this study, tetrasodium pyrophosphate decahydrate ($Na_4P_2O_7 \cdot 10H_2O$) was found to act as a nucleation catalyst for $CH_3CO_2Na \cdot 3H_2O$ which hardly lowers the melting point at all and does not diminish the heat of fusion.

We present the results of two different kinds of thermal analysis of $CH_3CO_2Na \cdot 3H_2O$ in the presence of $Na_4P_2O_7 \cdot 10H_2O$. One is a heating and cooling cycle of about 30 g samples in a sealed glass vessel, and the other is differential scanning calorimetry of about 15 mg samples. The reason why it acts as a nucleation catalyst for $CH_3CO_2Na \cdot 3H_2O$ is discussed crystallographically and compared to the well known case of borax ($Na_2B_4O_7 \cdot 10H_2O$) for Glawber's Salt ($Na_2SO_4 \cdot 10H_2O$).[3,6]

Experimental

Materials. $CH_3CO_2Na \cdot 3H_2O$, $Na_4P_2O_7 \cdot 10H_2O$, and $Na_2H_2P_2O_7$ were obtained commercially and $Na_4P_2O_7$ was obtained by heating $Na_4P_2O_7 \cdot 10H_2O$ in an oven at 150—200 °C for 5 h. $Na_4P_2O_7 \cdot 10H_2O$ was used for experiments after it was ground to a powder and passed through a 100 mesh seive.

Heating and Cooling Cycles of About 30 g Samples in a Sealed Glass Vessel. Weighed quantities of $CH_3CO_2Na \cdot 3H_2O$ and $Na_4P_2O_7 \cdot 10H_2O$ were placed in a glass vessel and the sample was covered with liquid paraffin to prevent water evaporation. The temperature of the sample was measured with a thermocouple, whose junction was placed near $Na_4P_2O_7 \cdot 10H_2O$ precipitates because it was expected that recrystallization of $CH_3CO_2Na \cdot 3H_2O$ would start on the surface of $Na_4P_2O_7 \cdot 10H_2O$ crystals. The glass vessel was sealed and put into a water bath. The sample was consecutively heated and cooled at the rate of 0.4 °C/min between 35 °C and 70 °C, and maintained for 30 min each at 35 °C and then 70 °C. In this manner, the melting point t_m and the temperature at which supercooling was broken t_i were measured and supercooling $\Delta t_i (= t_m - t_i)$ was determined in each cycle.

Differential Scanning Calorimetry. Differential scanning calorimetry (DSC) was performed using SSC 560S DSC (Dainiseikosha Co. Ltd.). Weighed quantities of samples were placed in a 15 μl silver crucible and the surface of the sample was covered with one drop of liquid paraffin to prevent water evaporation. The sample was subjected to linearly programmed consecutive heating and cooling in a manner similar to the above. Melting points t_m"s were obtained from the sample temperature curve at times corresponding to endothermal peaks and the temperatures at which supercooling was broken t_i"s were obtained from the sample temperature curves at times corresponding to the onset of exothermal peaks. From these temperatures, supercooling $\Delta t_i' (= t_m' - t_i')$ was calculated. This DSC system was calibrated using ice (t_m: 0.0 °C), sodium sulfate decahydrate (t_m: 32.4 °C) and sodium acetate trihydrate (t_m: 58.4 °C) as a standard.

Results

The heating and cooling curve for a sample consisting of 30 g of $CH_3CO_2Na \cdot 3H_2O$ and 0.3 g of $Na_4P_2O_7 \cdot 10H_2O$ is shown is Fig. 1. The curve shows that the melting point of this sample is 58.4 °C which is the same as that of $CH_3CO_2Na \cdot 3H_2O$ alone. The supercooling of the sample is broken at 53.1 °C and suddenly the temperature of the sample rises to freezing point, 58.4 °C. After this temperature is maintained for about 12 min, the temperature of sample drops.

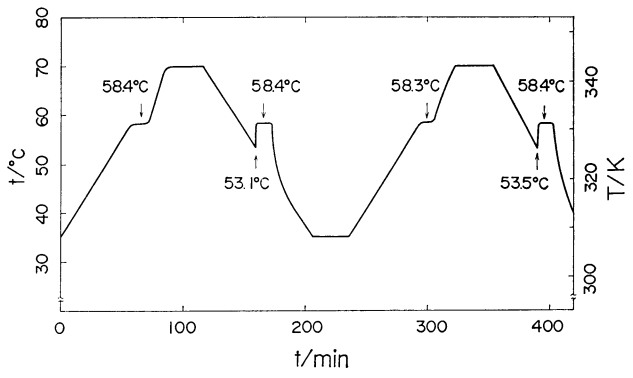

Fig. 1. Heating and cooling curve for a sample consisting of 30 g of $CH_3CO_2Na \cdot 3H_2O$ and 0.3 g of $Na_4P_2O_7 \cdot 10H_2O$.

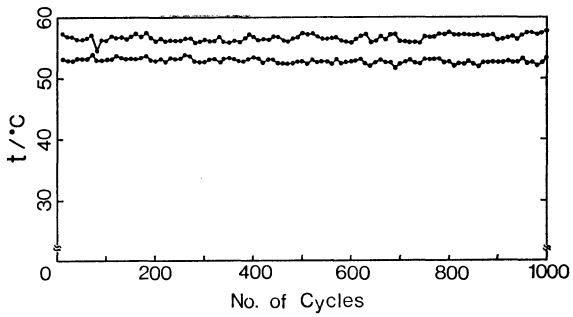

Fig. 2. Changes in melting point t_m and the temperature at which supercooling is broken t_i with cycling.
●: t_m, ○: t_i.

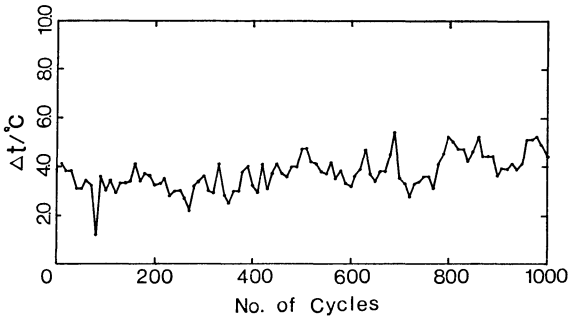

Fig. 3. Changes in supercooling Δt_i with cycling.

In this case, supercooling Δt_i is 5.3 °C.

The melting points t_m's and the temperatures at which supercooling is broken t_i's are plotted in Fig. 2, with temperature as ordinate and number of cycles as abscissa. As shown in Fig. 2, t_i and t_m are almost constantly 53 °C and 58.4 °C respectively. The slight scatter of t_m falls within measuring error. The supercooling Δt_i points are plotted in Fig. 3, using the result of Fig. 2. These Δt_i's are below 6 °C over all the cycles. It was also found that $Na_4P_2O_7 \cdot 10H_2O$ works continuously as a nucleation catalyst for 1000 cycles. On the other hand, when $Na_4P_2O_7 \cdot 10H_2O$ powder was not added to $CH_3CO_2Na \cdot 3H_2O$ melt, supercooling was not broken down to about 35 °C. These experimental results show that $Na_4P_2O_7 \cdot 10H_2O$ serves as a very effective nucleation catalyst for $CH_3CO_2Na \cdot 3H_2O$ whose melting point is scarcely lowered.

A DSC curve of a sample consisting of 14.0 mg of $CH_3CO_2Na \cdot 3H_2O$ and 1.7 mg of $Na_4P_2O_7 \cdot 10H_2O$ is illustrated in Fig. 4. The difference between the temperature of the first endothermal peak and that of the second is probably caused by measuring error. The melting points t_m"s and the temperatures at which supercooling is broken t_i"s which are determined by 50 continuous heating and cooling cycles are shown in Fig. 5. The supercooling in this case Δt_i"s ($=t_m' - t_i'$) are calculated by using the results of Fig. 5 and are plotted in Fig. 6. From Fig. 5, it is found that t_i' varies very widely and irregularly with number of cycles and their average is about 45 °C. Thus $\Delta t_i'$ also varies very widely and their average is 13 °C. It is evident that $\Delta t_i'$ is much larger than Δt_i. Moreover, the heat of fusion per 1 g of $CH_3CO_2Na \cdot 3H_2O$ which was obtained by this DSC measurement is 262

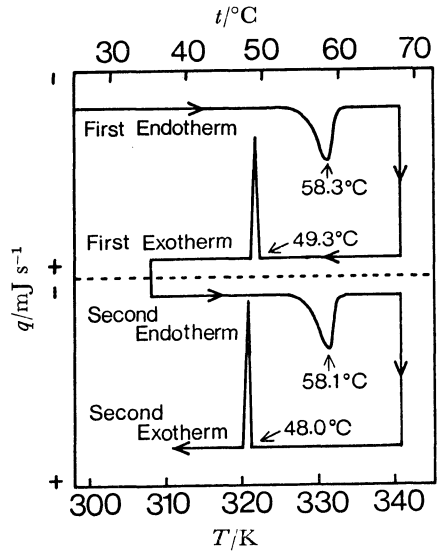

Fig. 4. DSC curve of a sample consisting of 14.0 mg of $CH_3CO_2Na \cdot 3H_2O$ and 1.7 mg of $Na_4P_2O_7 \cdot 10H_2O$.

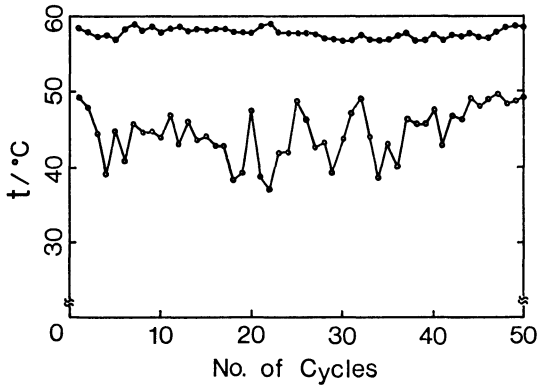

Fig. 5. Changes in melting point t_m' and the temperature at which undercooling is broken t_i' with cycling.
●: t_m', ○: t_i'.

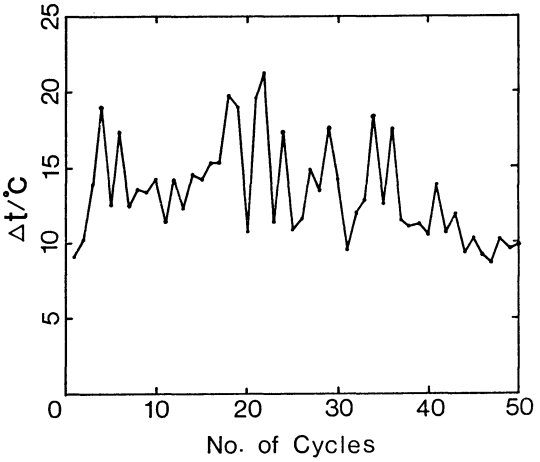

Fig. 6. Changes in undercooling $\Delta t_i'$ with cycling.

J/g, which is good agreement with that of $CH_3CO_2Na \cdot 3H_2O$ alone within measuring error. It is understandable that addition of $Na_4P_2O_7 \cdot 10H_2O$ to $CH_3CO_2Na \cdot 3H_2O$ scarcely decreases its heat of fusion.

The solubilities of $Na_4P_2O \cdot 10H_2O$ in $CH_3CO_2Na \cdot$

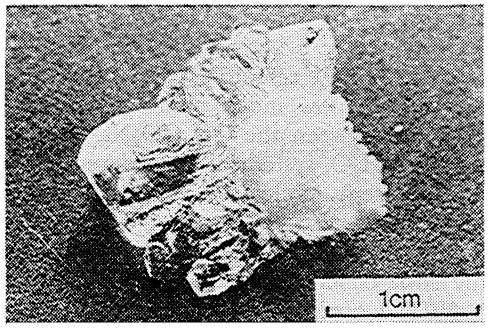

Fig. 7. Photograph of $CH_3CO_2Na \cdot 3H_2O$ crystals grown around a mass of $Na_4P_2O_7 \cdot 10H_2O$ polycrystal.

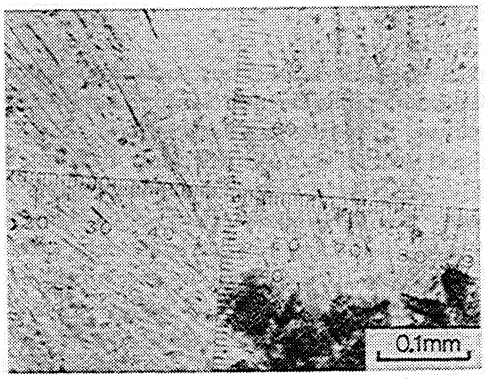

Fig. 8. Micro-photograph of $CH_3CO_2Na \cdot 3H_2O$ grown around $Na_4P_2O_7 \cdot 10H_2O$ particles.

$3H_2O$ melt at 60 °C and 75 °C were both about 0.1 percent by weight. Because of its slight solubility, it is supposed that both the melting point and the heat of fusion of $CH_3CO_2Na \cdot 3H_2O$ are hardly influenced by adding $Na_4P_2O_7 \cdot 10H_2O$. This is in good agreement with the results obtained by these thermal analyses.

Figure 7 shows $CH_3CO_2Na \cdot 3H_2O$ crystals grown around a mass of $Na_4P_2O_7 \cdot 10H_2O$ polycrystal. The white part indicates a mass of $Na_4P_2O_7 \cdot 10H_2O$ and transparent crystals around it are $CH_3CO_2Na \cdot 3H_2O$. Figure 8 is a micro-photograph of $CH_3CO_2Na \cdot 3H_2O$ crystals grown around $Na_4P_2O_7 \cdot 10H_2O$ particles. It is observed that $CH_3CO_2Na \cdot 3H_2O$ needles are radially grown from $Na_4P_2O_7 \cdot 10H_2O$ particles. It is suggested that $CH_3CO_2Na \cdot 3H_2O$ crystallized as needle since it began to recrystallize at a temperature significantly below the melting point. This large supercooling, we suppose, results from the small sample quantities of this experiment. This is consistent with the result obtained by DSC of about 15 mg sample.

Discussion

Table 1 shows the crystallographic data of $Na_2B_4O_7 \cdot 10H_2O$ and that of $Na_2SO_4 \cdot 10H_2O$,[7] and Table 2 shows the crystallographic data of $Na_4P_2O_7 \cdot 10H_2O$[8] and that of $CH_3CO_2Na \cdot 3H_2O$.[9] As shown in Table 1, the crystallographic data of $Na_2B_4O_7 \cdot 10H_2O$ and that of $Na_2SO_4 \cdot 10H_2O$ are quite similar except for a space group. Moreover, these two compounds have remarkably similar chains which are formed by sharing the two edges of $Na(H_2O)_6$ octahedra. These crystallographic similarities have been pointed out to be the cause of the nucleation catalysis.[7]

Table 1. Crystallographic data for sodium sulfate decahydrate and sodium tetraborate decahydrate

		$Na_2SO_4 \cdot 10H_2O$	$Na_2B_4O_7 \cdot 10H_2O$
Crystal system		Monoclinic	Monoclinic
Space group		$P2_1/c$	C2/c
Unit-cell parameter	a/Å	11.512	11.885
	b/Å	10.370	10.654
	c/Å	12.847	12.206
	β/°	107.789	106.623
	V/Å^3	1460	1481
	Z	4	4

Table 2. Crystallographic data for sodium acetate trihydrate and tetrasodium pyrophosphate decahydrate

		$CH_3CO_2Na \cdot 3H_2O$	$Na_4P_2O_7 \cdot 10H_2O$
Crystal system		Monoclinic	Monoclinic
Space group		C2/c	C2/c
Unit-cell parameter	a/Å	12.353	17.01±0.02
	b/Å	10.466	6.96±0.01
	c/Å	10.401	14.85±0.02
	β/°	111.69	112.0±0.2
	V/Å^3	1249.5	1630
	Z	8	4

On the other hand, both $Na_4P_2O_7 \cdot 10H_2O$ and $CH_3CO_2Na \cdot 3H_2O$ are monoclinic and have the same space group C2/c, however their lattice constants a, b, and c are greatly different. In the crystal structure of $CH_3CO_2Na \cdot 3H_2O$, Na ion has distorted octahedral coordination with six oxygen atoms which consist of one acetate oxygen and five water molecules. Adjacent octahedra share an edge and form a continuous chain along the z axis.[9,10] However, the crystal structure of $Na_4P_2O_7 \cdot 10H_2O$ contains two types of sodium atoms lying within octahedra, which are made up of six water molecules in the one case, and four water molecules and two oxygen atoms of a pyrophosphate group in the other case. The $Na(H_2O)_6$ octahedra share edges and corners with each other so as to build up sheets of linked octahedra. The other octahedron containing a pyrophosphate group shares two edges with the $Na(H_2O)_6$ octahedra so as to link to the sheets of $Na(H_2O)_6$ octahedra.[8,11] Thus it is deduced that the structures of $CH_3CO_2Na \cdot 3H_2O$ and $Na_4P_2O_7 \cdot 10H_2O$ do not have highly similar chains or sheets of water molecules-coordinate Na ions, whereas $Na_2SO_4 \cdot 10H_2O$ and $Na_2B_4O_7 \cdot 10H_2O$ have remarkably similar chains.

The lattice spacings on low index planes of $CH_3CO_2Na \cdot 3H_2O$ and $Na_4P_2O_7 \cdot 10H_2O$ which can be calculated from the lattice constants shown in Table 2 are listed in Table 3. In this table, the lattice spacings on planes of $Na_4P_2O_7 \cdot 10H_2O$ which agree with those of $CH_3CO_2Na \cdot 3H_2O$ within 1%, are written in the same row of those of $CH_3CO_2Na \cdot 3H_2O$. It can be seen that there are many planes of $CH_3CO_2Na \cdot 3H_2O$ whose lattice spacing is close to that of $Na_4P_2O_7 \cdot 10H_2O$.

TABLE 3. LATTICE SPACING ON LOW INDEX PLANES OF SODIUM ACETATE TRIHYDRATE AND THAT OF TETRASODIUM PYROPHOSPHATE DECAHYDRATE

$CH_3CO_2Na\cdot3H_2O$		$Na_4P_2O_7\cdot10H_2O$	
(*hkl*)	*d*/Å	*d*/Å	(*hkl*)
		15.77	(100)
		13.77	(001)
		13.08	(10$\bar{1}$)
(100)	11.48		
(010)	10.47		
(001)	9.665		
(10$\bar{1}$)	9.272		
		8.858	(101)
		8.317	(20$\bar{1}$)
		7.886	(200)
(110)	7.734		
		7.409	(10$\bar{2}$)
(011)	7.100		
(11$\bar{1}$)	6.940	6.960	(010)
		6.884	(002)
		6.540	(20$\bar{2}$)
(101)	6.330	6.368	(110)
		6.211	(011)
		6.144	(11$\bar{1}$)
(20$\bar{1}$)	6.004	5.949	(201)
(200)	5.739		
		5.670	(30$\bar{1}$)
		5.588	(102)
		5.473	(111)
(111)	5.416		
		5.338	(21$\bar{1}$)
(020)	5.233	5.257	(300)
(21$\bar{1}$)	5.208	5.228	(30$\bar{2}$)
(10$\bar{2}$)	5.193	5.218	(210)
(210)	5.032	5.073	(11$\bar{2}$)

For example, *d*(11$\bar{1}$) of $CH_3CO_2Na\cdot3H_2O$ agrees very closely with *d*(010) of $Na_4P_2O_7\cdot10H_2O$. Consequently, the reason why $Na_4P_2O_7\cdot10H_2O$ serves as an effective nucleation catalyst for $CH_3CO_2Na\cdot3H_2O$ is considered to be their close resemblance in lattice spacing on certain low index planes.

The extent of supercooling of $Na_2SO_4\cdot10H_2O$ containing $Na_2B_4O_7\cdot10H_2O$ is known to be 1—2 °C in the experiment using test tube[3] and 7 °C in DSC.[12] On the other hand, the extent of supercooling of $CH_3CO_2Na\cdot3H_2O$ containing $Na_4P_2O_7\cdot10H_2O$ is found to be about 5 °C in the experiment using sealed glass vessel and at an average of 13 °C in DSC. In each case, the extent of supercooling of $CH_3CO_2Na\cdot3H_2O$ containing $Na_4P_2O_7\cdot10H_2O$ is larger than that of $Na_2SO_4\cdot10H_2O$ containing $Na_2B_4O_7\cdot10H_2O$. As indicated before, $Na_2SO_4\cdot10H_2O$ and $Na_2B_4O_7\cdot10H_2O$ have analogous unit cells and remarkably similar chains which are formed by sharing two edges of $Na(H_2O)_6$ octahedra each other, whereas $CH_3CO_2Na\cdot3H_2O$ and $Na_4P_2O_7\cdot10H_2O$ only resemble each other in lattice spacing on certain low index planes. The difference of supercooling between the $CH_3CO_2Na\cdot3H_2O$ system and $Na_2SO_4\cdot10H_2O$ system is considered to be due to such a different modes of resemblance in crystal structure.

It was pointed out that there was difference between the supercooling of $Na_2SO_4\cdot10H_2O$ containing $Na_2B_4O_7\cdot10H_2O$ obtained by the heating and cooling cycles using sealed test tube and that obtained by using DSC.[13] The cause of this difference of supercooling extent for the $CH_3CO_2Na\cdot3H_2O$ system is not more clearly understood than for the $Na_2SO_4\cdot10H_2O$ system.

In addition, both anhydrous sodium pyrophosphate ($Na_4P_2O_7$) and sodium hydrogenpyrophosphates such as disodium dihydrogenpyrophosphate ($Na_2H_2P_2O_7$) were found to act as a nucleation catalyst as well as $Na_4P_2O_7\cdot10H_2O$. This effect comes from the fact that a part of $Na_4P_2O_7$ and $Na_2H_2P_2O_7$ become $Na_4P_2O_7\cdot10H_2O$ in $CH_3CO_2Na\cdot3H_2O$ melt. The presence of $Na_4P_2O_7\cdot10H_2O$ both in the mixture of 30 g of $CH_3CO_2Na\cdot3H_2O$ melt and 1 g $Na_4P_2O_7$ and in the mixture of 30 g of $CH_3CO_2Na\cdot3H_2O$ melt and 1 g of $Na_2H_2P_2O_7$ was confirmed by X-ray diffraction.

The authors wish to express their thanks to Dr. Ryoichi Kiriyama for his many helpful discussions and to Dr. Eiichi Hirota and Dr. Masanari Mikoda for their continuous encouragement. They are also grateful to Dr. Yoshihiro Matsuo for his discussions throughout this work, to Mr. Masahiro Nishikawa for his photography, and to Mr. Koji Matsunaga and Miss Fumiko Kimura for their thermal analyses.

References

1) M. Telkes, "Solar Materials Science," ed by L. E. Murr, Academic Press, New York (1980), Chap. 11.
2) F. de Winter, *Solar Energy*, **17**, 379 (1975).
3) M. Telkes, *Ind. Eng. Chem.*, **44**, 1308 (1952).
4) K. Narita and J. Kai, *J. Inst. Electr. Eng. Jpn.*, **101**, 15 (1981).
5) H. Kimura, *J. Jpn. Assoc. Cryst. Growth*, **7**, 215 (1980).
6) D. Turnbull and B. Vonnegut, *Ind. Eng. Chem.*, **44**, 1292 (1952).
7) H. A. Levy and G. C. Lisensky, *Acta Crystallogr., Sect. B*, **34**, 3502 (1978).
8) W. S. McDonald and D. W. J. Cruickshank, *Acta Crystallogr*, **22**, 43 (1967).
9) K. -T. Wei and D. L. Ward, *Acta Crystallogr., Sect. B*, **33**, 522 (1977).
10) T. S. Cameron, K. M. Mannan, and Md. O. Rahman, *Acta Crystallogr., Sect. B*, **32**, 87 (1976).
11) D. M. MacArthur and C. A. Beevers, *Acta Crystallogr.*, **10**, 428 (1957).
12) S. Cantor, *Thermochim. Acta*, **33**, 69 (1979).
13) M. Kamimoto, *Kagaku To Kogyo*, **33**, 598 (1980).